第 48 卷 第 12 期/2021 年 6 月/中国激光 研究论文

中国激光

基于 Yb:YAG 晶体衍生光纤的976 nm 单频激光器

谢永耀[1,2]，丛振华[1,2]，赵智刚[1,2]，张行愚[1,2]，赵显[3]，邵贤彬[1,2]，赵微[1,2]，刘兆军[1,2*]

[1]山东大学信息科学与工程学院，山东 青岛 266237；

[2]山东省激光技术与应用重点实验室，山东 青岛 266237；

[3]山东大学光学高等研究中心，山东 青岛 266237

摘要 采用熔融芯法制备出高增益的 Yb:YAG 晶体衍生光纤，纤芯内 Yb_2O_3 的掺杂浓度(质量分数)达到 5.25%。光纤在 976 nm 处的增益系数为 12.6 dB/cm，在 1550 nm 处的传输损耗为 1.29 dB/m。采用 DBR 线性腔结构，将 8 mm 长的 Yb:YAG 晶体衍生光纤作为增益光纤，实现了 17.8 mW 的 976 nm 单频激光输出，对应的斜效率为 12.1%，激光的信噪比大于 45 dB，线宽小于 41 kHz。

关键词 激光器；单频激光；光纤激光器；976 nm 激光；Yb:YAG 晶体；晶体衍生光纤

中图分类号 TN248 **文献标志码** A **doi**：10.3788/CJL202148.1201010

1 引 言

单频光纤激光器具有相干长度长、线宽窄、噪声低等优点，在相干光合束、引力波探测、激光雷达以及非线性频率变换领域有着良好的应用前景[1-4]。特别是波长为 976 nm 的单频激光器可以通过非线性频率变换获取蓝光以及紫外相干光源[5-6]，近年来受到广泛的关注；此外，相比于常规的 976 nm 半导体激光光源，其具有更低的噪声和更窄的线宽，还可用作超快激光器及放大器的低噪声泵浦源[7]。单频光纤激光器的实现方式主要有环形腔和线形腔结构。环形腔结构通常具有较长的激光腔长，为保证单频输出，往往需要在腔内插入滤波器件，这将引入额外的插入损耗，并且其结构复杂、单频稳定性差[8-10]。线形腔结构如布拉格反射式(DBR)结构，具有结构紧凑、稳定性高以及无跳模等优点，被广泛应用在单频光纤激光器中[11-13]。然而，这种 DBR 结构激光器的腔长通常被限制在几厘米以内，因此，为获得足够的增益来实现激光的高效输出，要求增益光纤具有较高的增益系数。

近年来，利用熔融芯法制备的新型 YAG 晶体衍生光纤因其新颖的特性引起了人们的关注，其产生的不同波段的激光特性也得到了广泛研究[14-18]。该光纤以 YAG 晶体为纤芯材料，纯石英管为包层材料，采用光纤拉丝塔在高温下进行拉丝。拉制过程中纤芯的 YAG 晶体材料由固态变为液态，与软化的玻璃包层发生扩散，并随着光纤的快速退火而凝固形成新的钇铝硅酸盐(YAS)玻璃纤芯，使得所制备的光纤具有非线性效应低、热导率高以及力学性能强等优点[19-20]。特别是纤芯中掺杂浓度相对较高的 Y 和 Al 元素，有效地抑制了稀土离子的浓度猝灭效应，使其比传统石英光纤具有更高的稀土掺杂浓度和更大的激光增益，有利于实现单频激光输出[21]。另外，相比于磷酸盐、锗酸盐等制成的软玻璃光纤，石英材料的外包层与商用石英光纤器件有更好的兼容性[22]。基于不同稀土掺杂的 YAG 晶体衍生光纤也成功用于获得 1 μm 波段的单频激光输出[23-25]。2019 年，华南理工大学的 Zhang 等[23]首次基于 Yb:YAG 陶瓷衍生特种光纤实现了 1064 nm 的单频激光输出，由于腔内损耗较大，激光

收稿日期：2021-02-18；**修回日期**：2021-03-16；**录用日期**：2021-03-24

基金项目：国家自然科学基金(62075117，62075116)、教育部联合基金(6141A02022430)、山东省重点研发计划(2019JMRH0111)、山东省自然科学基金(ZR2019MF039)、山东省自然科学基金青年基金(ZR2020QF095)、山东大学卓越团队基金、山东大学杰出中青年基金、山东大学齐鲁青年启动基金

*E-mail：zhaojunliu@sdu.edu.cn

器的斜效率为 3.8%。同年，本课题组通过减小 Yb∶YAG 晶体衍生光纤的纤芯直径来降低腔内损耗，获得了输出功率为 110 mW 的 1064 nm 单频激光，该激光器的斜效率为 18.5%[24]。然而，基于此类光纤的单频光纤激光器目前仅在 1 μm 波段得以实现，关于 1 μm 以下波段 YAG 晶体衍生光纤的研究鲜见报道。

本文基于熔融芯法制备出纤芯直径为 8.7 μm、外径为 125 μm 的 Yb∶YAG 晶体衍生特种光纤，并对其在 976 nm 处的激光特性进行研究。所制备光纤的纤芯内 Yb_2O_3 的质量分数为 5.25%，在 976 nm 处的增益系数约为 12.6 dB/cm。当 Yb∶YAG 晶体衍生光纤长度为1 cm 时，通过优化输出光栅反射率，976 nm 激光器的斜效率达到 24.3%。此外，采用 DBR 线形腔结构成功实现了线宽小于 41 kHz 的 976 nm 单频激光输出。所制备单频激光器的最高输出功率为 17.8 mW，激光信噪比大于 45 dB。

2　Yb∶YAG 晶体衍生光纤制备及表征

实验中纤芯的材料选择原子数分数为10% 的商用 Yb∶YAG 晶体，直径为 1.6 mm，经过抛光和清洗处理后，将其插入内径为 1.8 mm、外径为 10 mm 的高纯石英管中，制成光纤预制棒。光纤制备采用两次拉制的方法，首先，使用拉丝塔在约 2000 ℃高温下将预制棒拉制成直径为 1.7 mm 的棒状粗光纤，此时，由于石英包层和 YAG 晶体在高温下相互扩散，光纤纤芯材料不再是 YAG 晶体，而变为 YAS 玻璃态，这就会使其在二次拉制过程中熔点降低。然后，将一次拉制的粗光纤插入另一相同尺寸的高纯石英管中组成新的光纤预制棒，使用拉丝塔在约 1940 ℃温度下对其进行拉丝。通过精确控制送棒和拉丝速度，获得了外径为 125 μm 的 Yb∶YAG 晶体衍生特种光纤，光纤显微端面如图 1(a)插图所示，所制备光纤的纤芯和包层对比明显，且纤芯圆度较好，纤芯直径为 8.7 μm。

使用能谱分析仪(EDS；Thermo Scientific™ UltraDry)对所制备光纤的元素分布进行测量，结果如图 1(a)所示，受到扩散的影响，一部分 SiO_2 由包层进入纤芯中，其质量分数约为 58.83%，导致纤芯内原有的元素含量降低，其中 Al_2O_3、Y_2O_3 和 Yb_2O_3 的质量分数分别为16.32%、19.60% 和

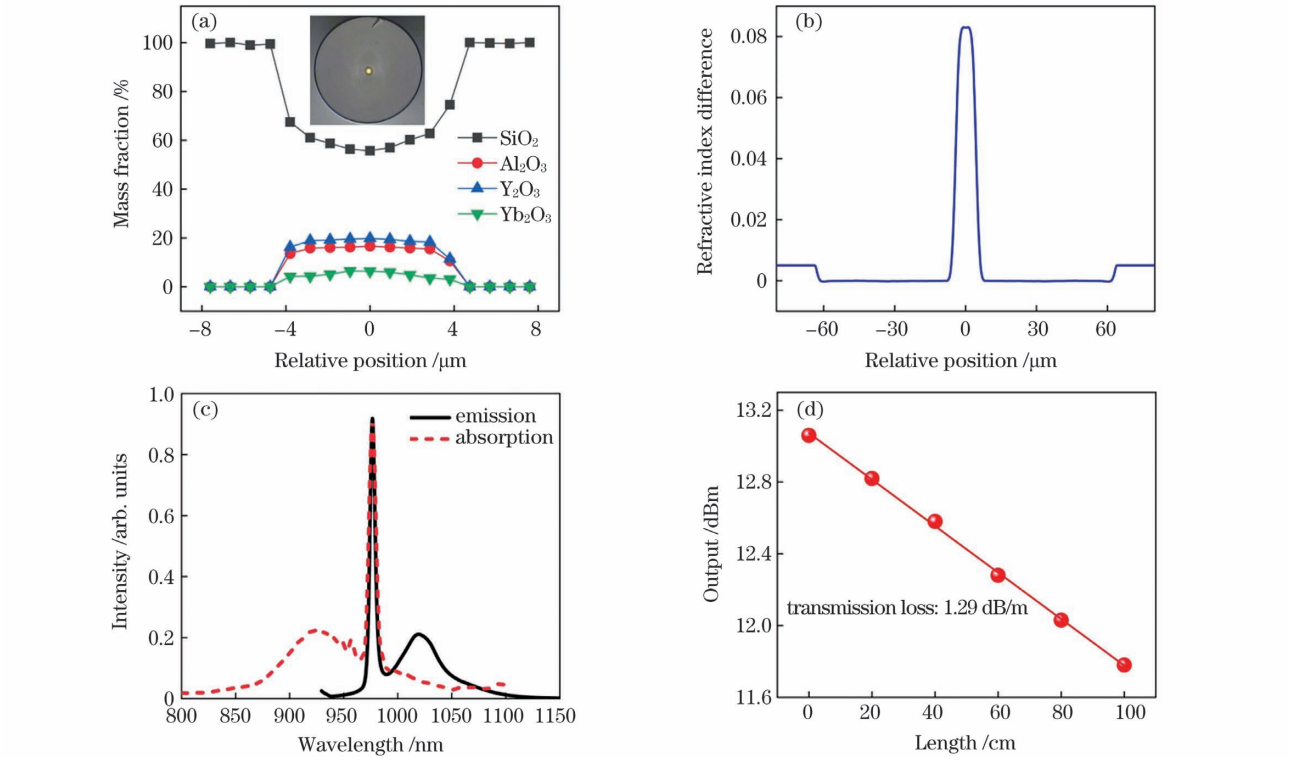

图 1　Yb∶YAG 晶体衍生光纤特性。(a)Yb∶YAG 晶体衍生光纤的元素分布，插图为光纤的光学显微端面；(b)光纤的折射率分布；(c)光纤的吸收光谱和发射光谱；(d)通过回切法测量的光纤在 1550 nm 处的传输损耗

Fig. 1 Characteristics of the Yb∶YAG crystal-derived fiber. (a) Composition distribution of the Yb∶YAG crystal derived silica fiber (YDSF), the insert is the optical micrograph of the fiber cross-section; (b) refractive index of the fiber; (c) absorption and emission spectra of the fiber; (d) transmission loss at 1550 nm measured by cut-back method

5.25%。图 1(b)所示为所制备光纤的折射率分布(SHR-1802),可以看到,折射率分布与元素分布基本一致,边缘呈渐变型分布,纤芯和包层的折射率差约为 0.083,对应的数值孔径约为 0.50。图 1(c)为所制备光纤的吸收光谱和发射光谱,从发射光谱可以看到,光纤在 976 nm 和 1030 nm 处具有较强的发射峰,对应于 Yb^{3+} 离子的 $^5F_{5/2}$ 至 $^5F_{7/2}$ 能级,因此 Yb:YAG 晶体衍生光纤可用作976 nm 和 1 μm 激光振荡器及激光放大器的增益光纤。从吸收光谱来看,Yb:YAG 晶体衍生光纤在915 nm 和 976 nm 处均有较强吸收,在 915 nm 和 976 nm 处的泵浦吸收系数分别达到 6 dB/cm 和 30 dB/cm,两个波长均可用作光纤激光器的泵浦波长。采用回切法对光纤传输损耗进行测量,由于 Yb^{3+} 掺杂光纤在 976 nm 处有较强的泵浦吸收作用,为避免光纤在 976 nm 波长处的吸收对传输损耗测量结果造成的影响,实验中选用 1550 nm 激光作为测试光源,实验结果如图 1(d)所示,所制备光纤在 1550 nm 处的传输损耗为 1.29 dB/m。

采用小信号放大系统对 Yb:YAG 晶体衍生光纤在976 nm 处的增益系数进行测量,实验装置如图 2(a)所示,所有器件均通过熔接方式进行连接。分别采用单模光纤耦合输出的 976 nm 半导体激光器(LD)及 915 nm LD 作为放大器的种子激光和泵浦光。通过波分复用器(WDM)将它们同时注入一段待测 YAG 晶体衍射光纤中进行放大,放大后的信号光经过一个带滤波器的 WDM 滤除残余泵浦光及 1 μm 处的自发辐射光(ASE)后输出,输出端接有隔离器(ISO),用来防止后向反射光对放大器的影响。实验中,分别采用功率为 0 dBm、3 dBm、5 dBm 的 976 nm LD 光源作为种子光,对长度分别为 1 cm 和 2 cm 的增益光纤的小信号增益进行测量。测量结果如图 2 所示。图 2(b)所示为光纤长度为 1 cm 时的测量结果,可以看到,当种子光功率为 0 dBm、泵浦光功率为 181 mW 时,光纤在 976 nm 处的增益系数达到 12.6 dB/cm,输出信号光光谱如图 2(b)插图所示,激光信噪比高于 30 dB。光纤长度为 2 cm 的测量结果如图 2(c)所示,其在 976 nm 处的最大增益系数为 8.1 dB/cm,相比于 1 cm 时的结果,增益系数有所降低,并且输出信号光的信噪比降低至 25 dB 左右,如图 2(c)插图所示。其原因主要是 Yb^{3+} 掺杂光纤在 976 nm 处的吸收系数较大,光纤长度增加,后面没有被充分泵浦的光纤会对 976 nm 激光进行重吸收,再以 ASE 形式进行发射,从而降低了光纤在 976 nm 处的增益系数,也造成了 976 nm 激光信噪比减小。

光纤在 976 nm 处的激光特性通过搭建线性激光谐振腔进行测试,泵浦方式采用纤芯泵浦。图 3(a)

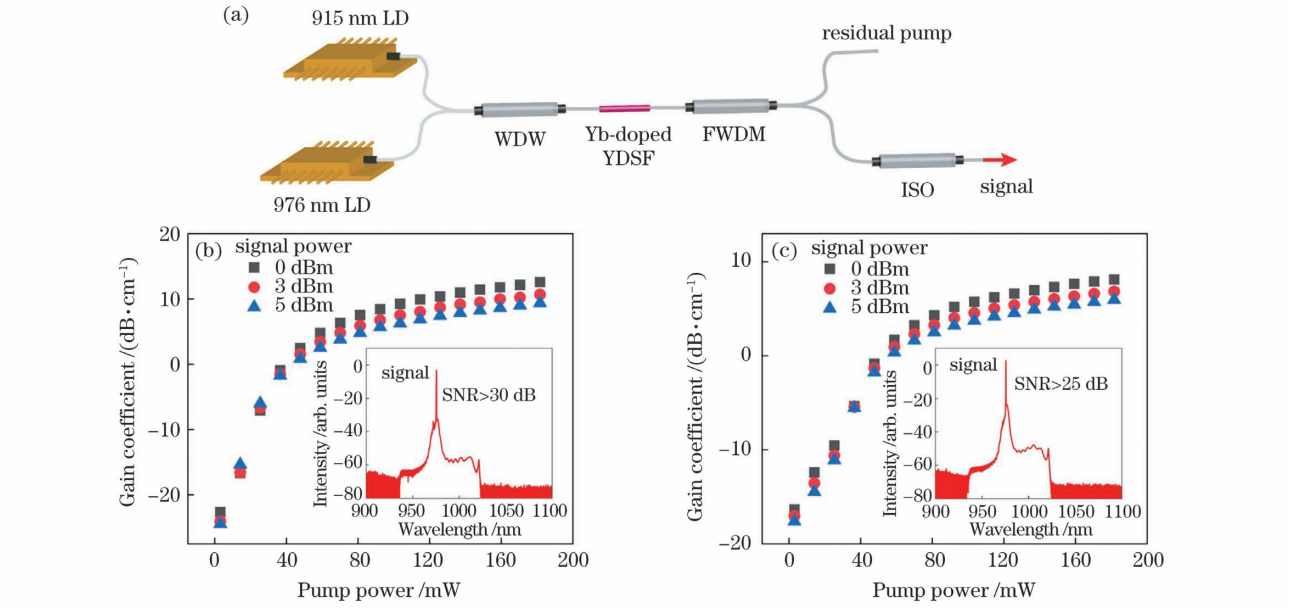

图 2 Yb:YAG 晶体衍生光纤在976 nm 处的增益特性。(a)基于 YDSF 的小信号放大器装置示意图;(b)光纤长度为 1 cm 和(c)光纤长度为 2 cm 时 YDSF 增益系数随泵浦功率的变化关系,插图均为在 181 mW 泵浦功率下输出信号光的光谱

Fig. 2 Gain characteristics of the Yb:YAG crystal-derived fiber at 976 nm. (a) The schematic of the amplifier setup based on the YDSF; the dependence of the gain coefficient of the YDSF on the pump power at (b) 1-cm YDSF and (c) 2-cm YDSF, the inserts are the signal output spectra of the amplifier at 181 mW pump power

为 976 nm 光纤激光器的结构示意图，激光谐振腔由一对高低反光纤布拉格光栅（FBG）及一段 Yb∶YAG 晶体衍生光纤组成。其中，低反光栅（LR-FBG）和高反光栅（HR-FBG）分别被刻写在商用保偏光纤（PM980）和普通单模光纤上（Hi1060），其栅区长度均为 1 cm。在高反光栅与增益光纤之间安装有偏振控制器（PC），用以控制腔内偏振状态，使腔内损耗达到最小。泵浦光为单模耦合的 915 nm LD 输出激光，通过保偏 WDM 后向泵浦注入谐振腔中，输出激光经保偏 ISO 后输出。实验中分别对不同长度的增益光纤及不同低反光栅的激光输出特性进行研究，实验结果如图 3 所示。首先对增益光纤长度进行优化，此时低反光栅的反射率选择为 60%，如图 3（b）所示，激光器在光纤长度为 2 cm、1 cm 和 0.5 cm 下获得的最高输出功率分别为 36.3 mW、37.2 mW 和 21.71 mW，对应的斜效率（SE）分别为 24.5%、24.3% 和 13.8%。为确保后续 DBR 线形腔激光器能够获得稳定的单频输出，当光纤长度为 1 cm 时，选择 3 种不同反射率的低反光栅对激光器的输出特性进行研究，结果如图 3（c）所示。与光栅反射率分别为 69% 和 84% 的激光输出相比，光栅反射率为 60% 时，在相同的泵浦功率下，976 nm 激光的输出特性更佳。

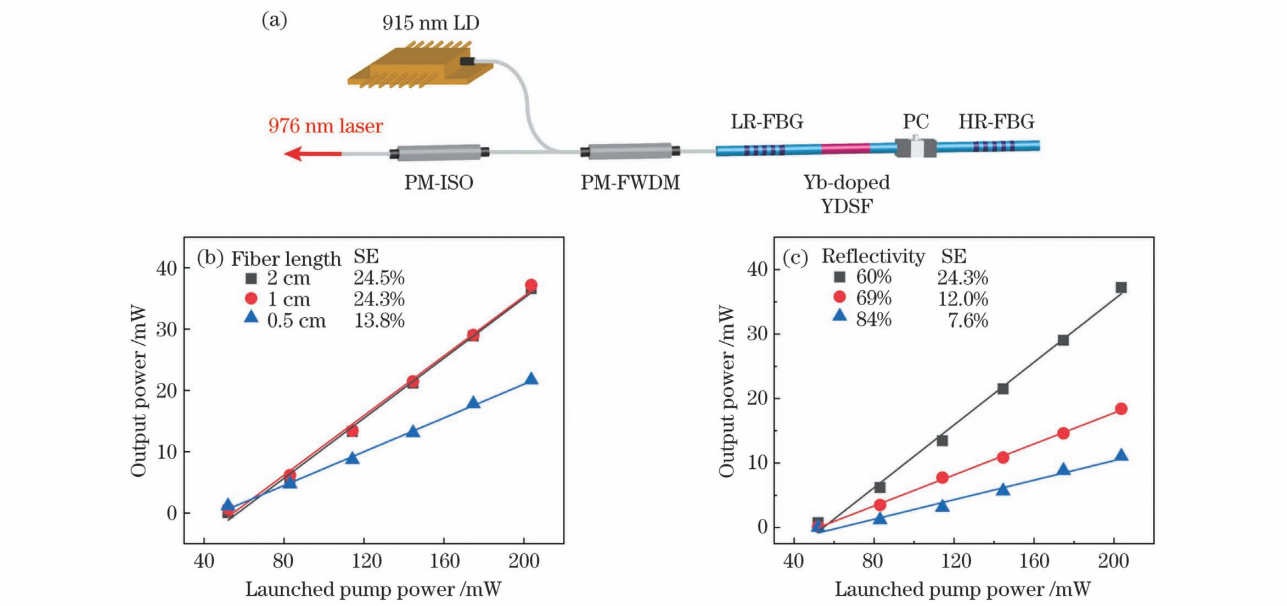

图 3　976 nm Yb∶YAG 晶体衍生光纤激光器的激光特性。（a）976 nm 光纤激光器结构示意图；（b）不同增益光纤长度和（c）不同输出光栅透过率（L_{YDSF}=1 cm）下 976 nm 激光器输出功率随注入泵浦功率变化

Fig. 3　Laser characteristics of 976-nm Yb∶YAG crystal-derived fiber laser. (a) The schematic of the fiber laser at 976 nm; the dependence of output power on the launched pump power with (b) various fiber lengths and (c) various reflectivities of 976 nm laser (L_{YDSF}=1 cm)

3　DBR 单频光纤激光器

基于 Yb∶YAG 晶体衍生光纤搭建了976 nm 单频光纤激光器，如图 4 所示。根据前面的实验结果，选择反射率为 60% 的低反光栅作为输出耦合器，反射带宽小于 0.05 nm，然后将 8 mm 长的 Yb∶YAG 晶体衍生光纤直接与高、低反光栅的栅区部分（尾纤长度小于 1 mm）进行熔接，以构成 DBR 激光谐振腔，并采用后向泵浦方式对其进行泵浦。整个激光腔被封装在铝块中，通过温度控制器对其进行精确的温度控制，温控器的控制精度为 0.01 ℃。同时，为了防止后向散射光对谐振腔的状态产生影响，

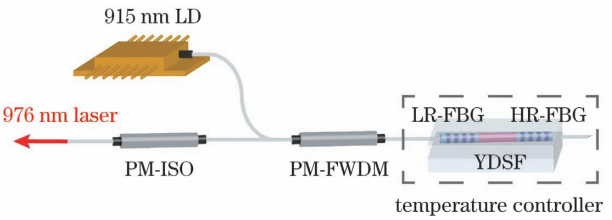

图 4　976 nm 线偏振单频 YDSF 光纤激光器结构示意图

Fig. 4　Linearly polarized single-frequency YDSF laser at 976 nm

PM-WDM 的输出端熔接有一个 PM-ISO，用以保证激光器的稳定性。

根据理论计算，激光谐振腔的有效腔长为 1.32 cm，对应的纵模间隔为 7.9 GHz[26]，大于低反

光栅反射带宽(15.7 GHz)的一半,因此腔内仅支持单个纵模运转。光纤激光器输出功率随注入泵浦功率的变化如图 5(a)所示,激光器的功率阈值约为 58 mW,当泵浦功率高于此阈值时,输出功率随泵浦功率线性增大。当注入泵浦功率为 203 mW 时,获得的最大输出功率为 17.8 mW,对应的斜效率为 12.1%。激光器的斜效率低于文献[5,27-28]中报道的 976 nm 单频激光器的斜效率,主要原因是所制备光纤的数值孔径大于目前商用光纤的数值孔径,Yb:YAG 晶体衍生光纤与光纤光栅之间的模式不匹配导致腔内损耗增大。另外,为保证激光器具有较大的单纵模区间,实验中所用的增益光纤长度为 0.8 cm,低于文献[5,27]中所用的光纤长度(L = 2 cm),导致残余泵浦功率增加,这也是造成效率较低的另一个重要因素。因此,需要进一步改进 Yb:YAG 晶体衍生光纤的性能,以提高激光器的效率,如通过添加高折射率的内包层来降低纤芯的数值孔径,通过减小扩散来提高纤芯的稀土掺杂浓度等。图 5(b)所示为 900~1100 nm 范围内测量的输出激光光谱,可以看到,976 nm 单频激光的信噪比大于 45 dB,且在光谱中未观察到来自 1 μm 波段的 ASE。图 5(b)插图所示为测量分辨率为 0.02 nm 时的激光光谱,输出激光的中心波长为 976.18 nm。激光器的光束质量如图 5(c)所示,x 和 y 方向的 M^2 因子分别为 1.01 和 1.02。图 5(c)插图为光斑的空间光束分布图,输出激光的光斑为标准的基横模分布。在谐振腔内激光振荡过程中,Yb:YAG 晶体衍生光纤的高阶模激光会进入单模光纤光栅包层中,相比于进入单模光纤光栅纤芯内的基横模激光,高阶模激光的腔内损耗较大,并在增益竞争的作用下被抑制,因此单频激光器的输出模式为基横模输出。

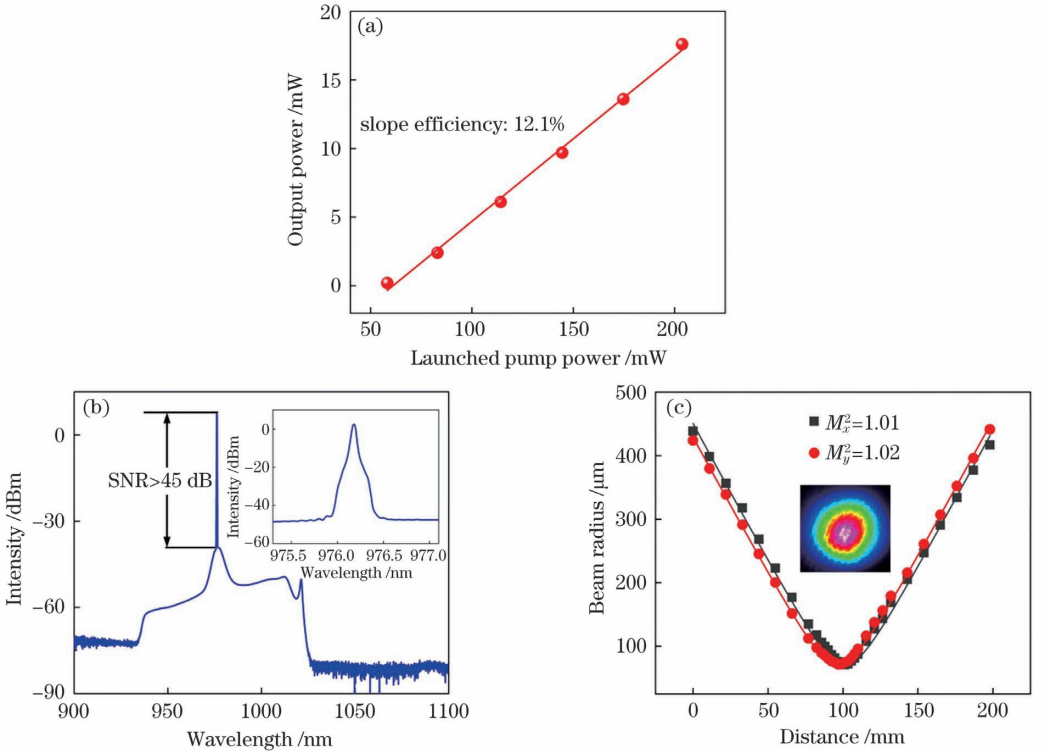

图 5 976 nm 单频光纤激光器的激光特性。(a)光纤激光器输出功率随注入泵浦功率变化;(b)900~1100 nm 范围内光纤激光器输出的激光光谱,插图为在分辨率为 0.02 nm 下测量的激光光谱;(c)单频光纤激光器的光束质量,插图为光斑的空间光束分布

Fig. 5 Laser characteristics of 976-nm single-frequency fiber laser. (a) Output power of the fiber laser with respect to the launched pump power; (b) output spectrum of the fiber laser from 900 nm to 1100 nm, the insert is the laser spectrum measured in 0.02 nm resolution; (c) beam quality of the single-frequency laser, the inset is the two-dimensional beam profile of the fiber laser

激光器的单纵模特性通过自行搭建的 Fabry-Perot(F-P)扫描干涉仪进行监测,该扫描干涉仪的自由光谱范围(FSR)为 3 GHz,分辨率为 19 MHz。图 6(a)所示为最高功率下的测量结果,通过精确地控制温度,激光器可以实现稳定的单纵模运转,通过 1 h 的监测,未发现跳模或模式竞争现象。采用延

时自外差法对单频激光器的线宽进行测量，测量系统使用 5 km 的单模光纤作为光纤延时线，对应的测量系统具有 41 kHz 的线宽测量分辨率[29]。最高输出功率下的测量结果如图 6(b)所示，对测量数据采用洛伦兹拟合，其 20-dB 线宽为 0.54 MHz，对应的 3-dB 激光线宽为 27 kHz。测量结果小于系统的测量分辨率，因此激光器的实际线宽应小于 41 kHz。

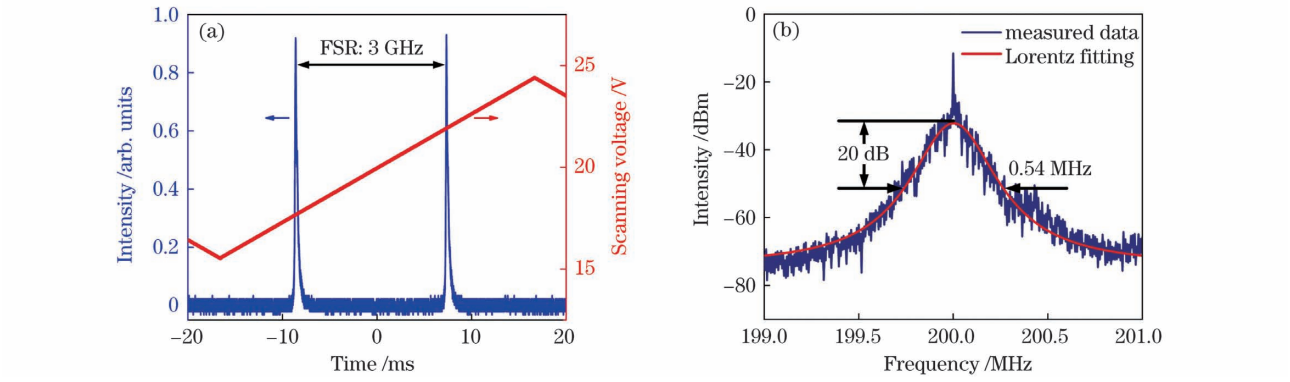

图 6　976 nm 单频光纤激光器的纵模和线宽特性。(a)F-P 扫描干涉仪测量的光纤激光器的纵模特性；(b)测量的单频光纤激光器的自外差信号及其洛伦兹拟合线宽

Fig. 6 Longitudinal mode and linewidth characteristics of 976 nm single-frequency fiber laser. (a) Longitudinal mode characteristics of the fiber laser measured by the scanning Fabry-Perot interferometer; (b) measured self-heterodyne signal of the single-frequency fiber laser with the Lorentzian fitted linewidth

4　结　　论

采用原子数分数为 10%的 Yb∶YAG 晶体作为纤芯前驱体材料，用熔融芯法制备了一种高增益的 Yb∶YAG 晶体衍生光纤，其纤芯内 Yb_2O_3 掺杂浓度(质量分数)达到 5.25%，并对其光学特性进行了研究。通过测量，发现所制备光纤在 915 nm 处的泵浦吸收系数达到 6 dB/cm，并且在 976 nm 处获得了高达 12.6 dB/cm 的放大增益系数。以 8 mm 长的 Yb∶YAG 晶体衍生光纤为增益介质，采用 DBR 结构实现了 17.8 mW 的 976 nm 单频激光输出。单频激光的信噪比大于 45 dB，激光线宽小于 41 kHz。实验结果还表明 Yb∶YAG 晶体衍生光纤是一种极具潜力的单频激光增益介质。

参　考　文　献

[1] Liu Z J, Zhou P, Xu X J, et al. Coherent beam combining of high power fiber lasers: progress and prospect[J]. Science China Technological Sciences, 2013, 56(7): 1597-1606.

[2] Abbott B P, Abbott R, Abbott T D, et al. GW151226: observation of gravitational waves from a 22-solar-mass binary black hole coalescence [J]. Physical Review Letters, 2016, 116(24): 241103.

[3] de Young R J, Barnes N P. Profiling atmospheric water vapor using a fiber laser lidar system [J]. Applied Optics, 2010, 49(4): 562-567.

[4] Georgiev D, Gapontsev V P, Dronov A G, et al. Watts-level frequency doubling of a narrow line linearly polarized Raman fiber laser to 589 nm[J]. Optics Express, 2005, 13(18): 6772-6776.

[5] Zhu X S, Shi W, Zong J, et al. 976 nm single-frequency distributed Bragg reflector fiber laser[J]. Optics Letters, 2012, 37(20): 4167-4169.

[6] Bouchier A, Lucas-Leclin G, Georges P, et al. Frequency doubling of an efficient continuous wave single-mode Yb-doped fiber laser at 978 nm in a periodically-poled $MgO:LiNbO_3$ waveguide [J]. Optics Express, 2005, 13(18): 6974-6979.

[7] Shi W, Fang Q, Zhu X S, et al. Fiber lasers and their applications[J]. Applied Optics, 2014, 53(28): 6554-6568.

[8] Chen J W, Zhao Y, Zhu Y N, et al. Narrow linewidth ytterbium-doped fiber ring laser based on saturated absorber[J]. IEEE Photonics Technology Letters, 2017, 29(5): 439-441.

[9] Ma X X, Lu B L, Wang K L, et al. Tunable broadband single-frequency narrow-linewidth fiber laser[J]. Acta Optica Sinica, 2019, 39(1): 0114001.
马选选，陆宝乐，王凯乐，等. 宽带可调谐单频窄线宽光纤激光器[J]. 光学学报，2019，39(1)：0114001.

[10] Wang X, Yan F P, Han W G. Single longitudinal mode narrow linewidth thulium-doped fiber laser with special subring cavity[J]. Chinese Journal of Lasers, 2019, 46(9): 0901001.
王雪，延凤平，韩文国. 基于特殊子环腔单纵模窄线

宽掺铥光纤激光器[J]. 中国激光, 2019, 46(9): 0901001.

[11] Spiegelberg C, Geng J H, Hu Y D, et al. Low-noise narrow-linewidth fiber laser at 1550 nm[J]. Journal of Lightwave Technology, 2004, 22(1): 57-62.

[12] Fang Q, Xu Y, Fu S, et al. Single-frequency distributed Bragg reflector Nd doped silica fiber laser at 930 nm[J]. Optics Letters, 2016, 41(8): 1829-1832.

[13] Yang C S, Cen X, Xu S H, et al. Research progress of single-frequency fiber laser [J]. Acta Optica Sinica, 2021, 41(1): 0114002.
杨昌盛, 岑旭, 徐善辉等. 单频光纤激光器研究进展[J]. 光学学报, 2021, 41(1): 0114002.

[14] Yoo S, Webb A S, Standish R J, et al. *Q*-switched neodymium-doped $Y_3Al_5O_{12}$-based silica fiber laser [J]. Optics Letters, 2012, 37(12): 2181-2183.

[15] Xie Y Y, Liu Z J, Cong Z H, et al. All-fiber-integrated Yb∶YAG-derived silica fiber laser generating 6 W output power[J]. Optics Express, 2019, 27(3): 3791-3798.

[16] Wan Y, Wen J X, Dong Y H, et al. Exceeding 50% slope efficiency DBR fiber laser based on a Yb-doped crystal-derived silica fiber with high gain per unit length[J]. Optics Express, 2020, 28(16): 23771-23783.

[17] Qian G, Wang W, Tang G, et al. Tm∶YAG ceramic derived multimaterial fiber with high gain per unit length for all-fiber mode-locked fiber laser applications[J]. Optics Letters, 2020, 45(5): 1047-1050.

[18] Tang G W, Qian G Q, Lin W, et al. Broadband 2 μm amplified spontaneous emission of Ho/Cr/Tm∶YAG crystal derived all-glass fibers for mode-locked fiber laser applications [J]. Optics Letters, 2019, 44(13): 3290-3293.

[19] Dragic P, Law P C, Ballato J, et al. Brillouin spectroscopy of YAG-derived optical fibers [J]. Optics Express, 2010, 18(10): 10055-10067.

[20] Ballato J, Hawkins T, Foy P, et al. On the fabrication of all-glass optical fibers from crystals[J]. Journal of Applied Physics, 2009, 105(5): 053110.

[21] Dragic P D, Cavillon M, Ballato J. Materials for optical fiber lasers: a review [J]. Applied Physics Reviews, 2018, 5(4): 041301.

[22] Li C Z, Jia Z X, Cong Z H, et al. Gain characteristics of ytterbium-doped SiO_2-Al_2O_3-Y_2O_3 fibers[J]. Laser Physics, 2019, 29(5): 055804.

[23] Zhang Y M, Wang W W, Li J, et al. Multi-component yttrium aluminosilicate (YAS) fiber prepared by melt-in-tube method for stable single-frequency laser[J]. Journal of the American Ceramic Society, 2019, 102(5):2551-2557.

[24] Liu Z, Xie Y, Cong Z, et al. 110 mW single-frequency Yb∶YAG crystal-derived silica fiber laser at 1064 nm[J]. Optics Letters, 2019, 44(17): 4307-4310.

[25] Xie Y Y, Cong Z H, Zhao Z G, et al. Linearly polarized single-frequency fiber laser based on the Yb∶YAG-crystal derived silica fiber [J]. Applied Optics, 2020, 59(32): 9931-9935.

[26] Barmenkov Y O, Zalvidea D, Torres-Peiró S, et al. Effective length of short Fabry-Perot cavity formed by uniform fiber Bragg gratings[J]. Optics Express, 2006, 14(14): 6394-6399.

[27] Fang Q, Shi W, Tian X P, et al. 978 nm single frequency actively *Q*-switched all fiber laser [J]. IEEE Photonics Technology Letters, 2014, 26(9): 874-876.

[28] Huang Z P, Deng H Q, Yang C S, et al. Self-injection locked and semiconductor amplified ultrashort cavity single-frequency Yb^{3+}-doped phosphate fiber laser at 978 nm[J]. Optics Express, 2017, 25(2): 1535-1541.

[29] Horak P, Loh W H. On the delayed self-heterodyne interferometric technique for determining the linewidth of fiber lasers[J]. Optics Express, 2006, 14(9): 3923-3928.

A 976-nm Single-Frequency Laser Based on the Yb∶YAG Crystal-Derived Fiber

Xie Yongyao[1,2], Cong Zhenhua[1,2], Zhao Zhigang[1,2], Zhang Xingyu[1,2], Zhao Xian[3], Shao Xianbin[1,2], Zhao Wei[1,2], Liu Zhaojun[1,2*]

[1] *School of Information Science and Engineering, Shandong University, Qingdao, Shandong* 266237, *China*;

[2] *Shandong Provincial Key Laboratory of Laser Technology and Application, Qingdao, Shandong* 266237, *China*;

[3] *Center for Optics Research and Engineering, Shandong University, Qingdao, Shandong* 266237, *China*

Abstract

Objective Single-frequency fiber lasers (SFFLs) are widely used in areas of coherent beam combination, gravitational wave detection, lidar, and nonlinear frequency conversion because of their excellent performance. In particular, SFFLs operating at 976 nm are highly demanded for nonlinear wavelength conversion to generate coherent blue light. SFFLs use either a ring- or linear-cavity configuration. The ring-cavity setup is complicated because many additional components must be inserted to enable a single-frequency output, which unavoidably introduces insertion loss. In addition, the stable single-frequency operation of a ring-cavity fiber laser is susceptible to environmental changes and vibrations, thereby resulting in mode hopping. In comparison, linear-cavity construction, such as the distributed Bragg reflector (DBR) scheme, is more compact, which creates a large longitudinal mode spacing, helping to maintain lasing on a stable single longitudinal and hop-free mode. The cavity length of DBR SFFL is limited to only a few centimeters. Therefore, high-gain fibers are demanded to enable sufficiently high gain. A novel Yb∶YAG crystal-derived fiber (YDSF) that exhibits some unique properties in fiber lasers has been developed. The YDSF was fabricated based on a molten core method (MCM) and shows advantages such as high doping levels and high stimulated Brillouin scattering threshold. In addition, the pure silica cladding of the YDSF makes it highly compatible with commercially available silica fiber devices. All the above mentioned characteristics make the YDSF suitable for high-power single-frequency lasers. Based on these fibers, single-frequency lasers emitting at 1 μm have been demonstrated recently. In 2019, we demonstrated a 110-mW single-frequency YDSF laser at 1064 nm. However, to the best of our knowledge, single-frequency YDSF lasers below 1 μm have never been reported.

Methods A commercially available 10% (atomic number fraction) Yb∶YAG crystal was used to prepare a YDSF. In the experiment, the entire preparation process was divided into two steps to maintain the uniformity of the optical fiber. First, a rod fiber having a diameter of ~1.7 mm was fabricated using a 1.6-mm YAG crystal and pure silica tube (D_{inner} = 2 mm, D_{external} = 10 mm). The drawing temperature was controlled at ~2000 ℃. Second, the YDSF was fabricated based on the rod fiber. A short piece of rod fiber was inserted into a different silica tube with the same specification to constitute a new preform, which was drawn into the fiber at 1940 ℃. Next, the physical and optical properties of the YDSF were measured using some devices and methods, such as an optical microscope, energy dispersive spectrometer, fiber refractometer, and cut-back method. Afterward, a homemade all-fiber amplifier was used to measure the gain coefficient of the YDSF at 976 nm. Then, the laser performance of the YDSF was investigated by optimizing the gain-fiber length and reflectivity of fiber Bragg grating (FBG). In addition, a DBR SFFL based on an 8-mm-long YDSF was built to further verify the performance of the YDSF.

Results and Discussions The mass fraction of SiO_2 and Yb_2O_3 in the core region of the YDSF were measured to be 58.83% and 5.25%, respectively (Fig. 1). As expected, interdiffusion occurred between the Yb∶YAG core and silica cladding during the drawing process. The refractive index profile of the fiber cross section was measured; the numerical aperture (NA) of the core with a diameter of 8.7 μm was 0.5 (Fig. 1), indicating that the YDSF was a multimode fiber. The absorption peaks of the YDSF were located at 915 nm and 976 nm, corresponding to the transitions from the ground state $^2F_{7/2}$ to higher states of $^2F_{5/2}$ of Yb^{3+}. The peak absorption coefficients were 6 dB/cm and 30 dB/cm for 915 nm and 976 nm, respectively (Fig. 1). For a signal power of 0 dBm and pump power of 181 mW, the net gain coefficient of the YDSF reached 12.6 dB/cm (Fig. 2), which indicated that the YDSF could be used as a gain medium for a 976-nm laser. By optimizing the gain-fiber length and reflectivity of FBG, a maximum output power of 37.2 mW was obtained with a slope efficiency of 24.3% (Fig. 3). In addition, using the 8-mm-long

YDSF as the gain medium, a 976-nm DBR SFFL was demonstrated. A maximum output power of 17.8 mW with a signal-to-noise ratio (SNR) of >45 dB was obtained at a launched pump power of 203 mW, and no output power saturation was observed. The corresponding slope efficiency was 15.1% (Fig. 5), which was low because of the mode mismatch. More efforts should be made for reducing the NA and improving Yb^{3+} doping concentration. The linewidth of the laser was measured to be less than 41 kHz, which was limited by the measurement setup (Fig. 6). The beam quality of the laser output was also measured using a charge-coupled device (Thorlabs, BC106N-VIS); the beam quality factor was measured to be 1.01 and 1.02 in the horizontal and vertical directions, respectively (Fig. 5).

Conclusions A YDSF with 5.25% Yb_2O_3 doping concentration (mass fraction) was fabricated using MCM. The transmission loss of the YDSF with a core diameter of 8.7 μm was measured to be 1.29 dB/m at 1550 nm. The gain coefficient of the YDSF was 12.6 dB/cm at 976 nm with a pump absorption coefficient of 6 dB/m at 915 nm. Using the DBR linear cavity, a 17.8-mW single-frequency laser at 976 nm was achieved with an 8-mm-long YDSF, exhibiting a slope efficiency of 18.5%. To the best of our knowledge, this is the first demonstration of a single-frequency YDSF laser below 1 μm. The SNR was measured to be >45 dB with a linewidth of less than 41 kHz. Results indicate that the YDSF is a promising candidate material for the SFFL operating in the 976-nm wavelength region.

Key words lasers; single-frequency laser; fiber lasers; 976 nm laser; Yb∶YAG crystal; crystal-derived fiber

OCIS codes 140.3570; 060.3510; 140.3410; 060.2280